

This work was written as part of one of the author's official duties as an Employee of the United States Government and is therefore a work of the United States Government. In accordance with 17 U.S.C. 105, no copyright protection is available for such works under U.S. Law. Access to this work was provided by the University of Maryland, Baltimore County (UMBC) ScholarWorks@UMBC digital repository on the Maryland Shared Open Access (MD-SOAR) platform.

Please provide feedback

Please support the ScholarWorks@UMBC repository by emailing scholarworks-group@umbc.edu and telling us what having access to this work means to you and why it's important to you. Thank you.

Coherence length for second-harmonic generation in nonlinear, one-dimensional, finite, multilayered structures

Nadia Mattiucci

Time Domain Corporation, Cummings Research Park, 7057 Old Madison Pike, Huntsville, Alabama 35806 and Charles M. Bowden Research Facility, Building 7804, U.S. Army Research, Development, and Engineering Command, Redstone Arsenal, Alabama 35898-5000, USA

Giuseppe D'Aguanno, Michael Scalora, and Mark J. Bloemer

Charles M. Bowden Research Facility, Building 7804, U.S. Army Research, Development, and Engineering Command, Redstone Arsenal, Alabama 35898-5000, USA

Received May 22, 2006; revised November 16, 2006; accepted November 20, 2006;
posted November 30, 2006 (Doc. ID 71161); published March 15, 2007

We find an analytic expression for second-harmonic conversion efficiency (both forward and backward) in generic, 1D, finite, multilayered structures, where the respective roles of effective phase-matching conditions and field overlap are clearly identified. Our approach places the notions of effective index and effective phase-matching conditions on a more solid theoretical ground and clarifies the meaning and the limits of applicability of these concepts. We also define a coherence length for the process in an unambiguous way and point out similarities and differences with the coherence length that is usually defined for bulk materials. Finally, we address the role played by absorption and provide numerical examples that confirm the analytical results found. © 2007 Optical Society of America

OCIS codes: 190.2620, 310.6860.

1. INTRODUCTION

Structures in which scattering or diffracting elements are arranged in such a way that their mutual distances are comparable with the wavelength of the incident wave are often referred to as photonic crystals (PCs), or photonic bandgap structures (PBGs). Typically, photonic crystals are periodic or quasi-periodic arrays in 1D, 2D, or 3Ds. PSGs are able to selectively transmit or reflect light at various wavelengths, as they affect the properties of the light in almost the same way that semiconductor crystals affect the properties of electrons. A periodic arrangement of different dielectric materials results in allowed and forbidden frequency bands and gaps for the incident light, analogous to energy bands and gaps of semiconductors.¹ The name “photonic crystal” and the exciting growth of PC research have their origins with the works of Yablonovitch² and John,³ in the late 1980s. They began by exploring basic theoretical concepts and by performing experiments in the microwave regime, where 3D structures could easily be fabricated.

One-dimensional photonic crystals (1D PCs), also known as 1D photonic bandgap structures, Bragg gratings, or more simply as multilayered structures, represent the simplest example of a photonic bandgap structure. Despite their simplicity, they retain many of the characteristics that can be found in more complicated, higher-dimensional topologies. One-dimensional PBGs

are made of alternating layers of all-dielectric materials, or alternating layers of metallic and dielectric materials. The fact that 1D PCs had great potential had already been anticipated in the seminal work of Bloembergen and Sievers,⁴ back in 1970. Although they considered infinite structures, the results they obtained have general validity: They showed that the periodicity of the layered structure can be used to compensate the normal dispersion of materials in order to obtain high conversion efficiency through phase-matched second-order interactions. Nevertheless, PCs are intrinsically finite, and even for the simplest linear, 1D case, it is still not clear how to distill into a simple compact formula the competing roles played by phase-matching conditions and field localization in a second-harmonic (SH) generation process. Recently, Centini *et al.*⁵ introduced the concept of effective index (n_{eff}) for 1D PCs that described the effective, dispersive properties of the structure. The concept of the effective index originates from a simple idea: One assumes that a multilayer structure, composed of several alternating layers of materials with different refractive indices and material dispersion, may be described by an effective index of refraction, which simultaneously folds material and geometrical dispersion into a single parameter n_e , the effective index of refraction. Then, a plane wave propagating through this hypothetical material will experience a phase and an amplitude change as follows:

$$\frac{E_f}{E_i} = \exp[i \operatorname{Re}(k_e)L - \operatorname{Im}(k_e)L], \quad (1)$$

where E_i is the complex amplitude of the electric field incident on the medium and E_f is the complex amplitude of the electric field at the structure's exit. $\operatorname{Re}(k_e)$ and $\operatorname{Im}(k_e)$ are the respective real and imaginary parts of the effective wave vector, defined by $k_e = n_e \omega / c$, where n_e is the complex effective index of the structure. Now, by using the definition of the complex transmission t , we also have

$$\frac{E_f}{E_i} = t = \sqrt{T} \exp[i\varphi], \quad (2)$$

where $T = |t|^2$ is the transmittance and φ is the normalized phase of the transmission. Combining Eqs. (1) and (2) yields the following definition of the complex effective index n_e (Ref. 5):

$$n_e = n_{\text{eff}} + i\beta_{\text{eff}} = \frac{c}{\omega L} [\varphi - i \ln(\sqrt{T})], \quad (3)$$

where the phase of the transmission φ must be a continuous function of the frequency ω and must satisfy the condition that $\varphi \rightarrow 0$ when $\omega \rightarrow 0$.⁵

This definition of effective index has been successfully used to find phase-matching conditions for the enhancement of nonlinear interactions, both theoretically and experimentally. Earlier numerical work⁶ had already established that specific tuning conditions resulted in high second-harmonic conversion efficiency. The effective index approach developed in Ref. 5 then showed that the higher conversion efficiency found in Ref. 6 coincided with perfect phase matching in terms of the effective index, namely, $n_{\text{eff}}(\omega) = n_{\text{eff}}(2\omega)$. After this realization, the effective index approach was used theoretically^{7–9} and experimentally^{10–12} to study and optimize SH generation in 1D PCs. In addition, the effective index has been used to find simultaneous phase-matching conditions for second and third-harmonic generation in $\chi^{(2)}$ -doped crystals¹³; the design of optical components¹⁴; and, more recently, in the development of a second quantization theory in 1D PCs.¹⁵ Until recently, it was thought that effective phase-matching conditions should provide a recipe for optimized, nonlinear conversion efficiency. However, it has been shown that¹⁶ in some cases a phase mismatch between the fundamental and second-harmonic fields can lead to higher conversion efficiencies compared to the phase-matched case.^{5,6} Under the circumstances described in Ref. 16, the benefits of field localization effects can outweigh any benefits that might arise from phase-matching conditions. Although it had been already demonstrated in Refs. 17–19 that the overlap integrals of the fundamental frequency (FF) and SH modes inside the structure play key roles in the enhancement of the SH process in 1D, finite photonic crystals, it is still not clear how effective phase-matching conditions affect the SH generation process. In view of these considerations and apparent shortcomings, we will seek to further clarify the concept of phase matching in layered structures. This will lead to an analytical expression for the SH conversion efficiency from which will stem two unambiguous, impor-

tant concepts: a coherence length for layered structures, and effective phase-matching conditions. In the outcome, we will also be able to distinguish between the role by the field localization versus that played by the phase-matching conditions in the enhancement of the SH generation process.

2. EFFECTIVE INDEX AND COHERENCE LENGTH FOR THE SECOND HARMONIC GENERATION PROCESS

Let us start by discussing some basic properties of both the transmission and the effective index of refraction when a generic structure A , which we can think of as a “building block,” is repeated N times, and let us indicate with A^N the structure repeated N times. One can show that the transmission resonances of the structure A are also transmission resonances for any N -period structure A^N , and that the effective index calculated for the structure A is the same for the N -period structure. To demonstrate this statement we begin with the Helmholtz equation for the electric field, under the assumption of plane, monochromatic waves, at normal incidence along the propagation direction z :

$$\frac{d^2 E}{dz^2} + \frac{\omega^2}{c^2} \varepsilon(z) E = 0, \quad (4)$$

where $\varepsilon(z)$ is the space-dependent, complex, dielectric permittivity of the structure A .

The boundary conditions require that the electric field E and its derivative dE/dz be continuous at the input and output interfaces of the structure.²⁰ Now, let us assume that A admits a transmission resonance at a given frequency ω , where the reflection $r_{\omega,A} = 0$ and the transmission $t_{\omega,A} = \sqrt{T_{\omega,A}} \exp[i\varphi_{\omega,A}]$ (in the case of a nonabsorbing structure, $\sqrt{T_{\omega,A}} = 1$), then for left-to-right (LTR) incidence we have: $E_{\text{in}} = 1$, $dE_{\text{in}}/dz = i n_0 \omega / c$, and $E_{\text{out}} = t_{\omega,A}$, and $dE_{\text{out}}/dz = i n_0 \omega / c t_{\omega,A}$, where E_{in} and dE_{in}/dz are the values of the field and its derivative taken at the input interface, E_{out} and dE_{out}/dz are the corresponding values at the output interface, and n_0 is the index of refraction of the external medium that surrounds the structure. When a second building block A is added to the structure, the boundary conditions at the input interface of the second structure will be just scaled by a constant factor $t_{\omega,A}$ with respect to the boundary conditions at the input interface of the first structure. Therefore the electric field inside the second structure is proportional to the electric field inside the first structure by a factor of $t_{\omega,A}$. Now, if L is the length of building block A , we have that: $E(z+L) = t_{\omega,A} E(z)$, and the transmission at the output of the A^2 structure is $t_{\omega,A}^2 = (\sqrt{T_{\omega,A}} \exp[i\varphi_{\omega,A}])^2$ (see Fig. 1 for a schematic). One may then repeat the same arguments for each additional building block, and for an N -period structure we have

$$t_{\omega,NA} = (t_{\omega,A})^N = (\sqrt{T_{\omega,A}} \exp[i\varphi_{\omega,A}])^N, \quad (5)$$

$$\Phi_{\omega,NA}^+(z + jL) = t_{\omega,A}^j \Phi_{\omega,NA}^+(z), \quad (6)$$

where, $t_{\omega,NA}$ is the transmission of the N -period structure, while $t_{\omega,A}$, $T_{\omega,A} = |t_{\omega,A}|^2$, and $\varphi_{\omega,A}$ are, respectively, the

transmission, the transmittance, and the normalized phase of the transmission of the building block A at the frequency ω . In Eq. (6), $\Phi_{\omega,NA}^+$ is the LTR mode of the whole structure at the frequency ω , i.e., it is the linear field in the structure calculated from Eq. (4) using an input plane wave of unitary amplitude incident from left to right. More details about the LTR and right-to-left (RTL) modes can be found in Refs. 21–23, for example.

If we now calculate the effective index at the frequency ω for building block A ($n_{e,A}^\omega$) and for the N -period structure ($n_{e,NA}^\omega$) using Eqs. (3) and (5), we find that

$$\begin{aligned} n_{e,NA}^\omega &= \frac{c}{\omega l} [\varphi_{\omega,NA} - i \ln(\sqrt{T_{\omega,NA}})] = \frac{c}{\omega L} [\varphi_{\omega,A} - i \ln(\sqrt{T_{\omega,A}})] \\ &= n_{e,A}^\omega = n_e^\omega. \end{aligned} \quad (7)$$

For right-to-left (RTL) incidence one has a parallel situation, and by using similar arguments one can show that

$$\Phi_{\omega,NA}^-(z + jL) = t_{\omega,A}^{-j} \Phi_{\omega,NA}^-(z), \quad (8)$$

where $\Phi_{\omega,NA}^-$ is the RTL mode of the structure at the frequency ω .

Equation (8) is a consequence of the fact that the RTL and LTR transmissions are equal in amplitude and in phase in all cases.^{20,21} The minus sign in the power of the scaling factor is due to the fact that the phase of the field in the RTL incidence case accumulates in the opposite way with respect to that of the field incident from LTR.

The above discussion leads to the conclusion that if the pump and the SH beams are both tuned at a transmission resonance of structure A , then any periodic structure A^N

will have the same effective index and the same phase-matching conditions as those of the basic structure A .

Let us now calculate the forward and backward conversion efficiencies (η^+ and η^- , respectively) in the nondepleted pump approximation for the A^N structure. Using a rigorous 1D Green's function approach,^{21,22} the conversion efficiency (η) may generally be linked to the LTR and RTL modes of the structure with the following expression²³:

$$\begin{aligned} \eta &= \eta^+ + \eta^- = \frac{2\omega^2 l^2}{\varepsilon_0 c^3} \left(\left| \frac{1}{l} \int_0^l d^2(z) [\Phi_{\omega,NA}^+(z)]^2 \Phi_{2\omega,NA}^-(z) dz \right|^2 \right. \\ &\quad \left. + \left| \frac{1}{l} \int_0^l d^2(z) [\Phi_{\omega,NA}^+(z)]^2 \Phi_{2\omega,NA}^+(z) dz \right|^2 \right) I_\omega^{\text{input}}, \end{aligned} \quad (9)$$

where $l = NL$ is the length of the structure and $d^2(z)$ is its spatial-dependent quadratic coefficient. We note that the forward and backward conversion efficiencies are linked to the overlap integrals that in the case of resonance tuning are essentially equal to the overlap integrals that had previously been calculated in Ref. 17. We also note that in the above formulas, the effective index never appears explicitly. Now, because we are supposing that our structure is made by repeating the basic building block N times, we can separate the integral into a sum of integrals each carried out over a basic the unit cell A . Now, taking into account the relations between the electric fields inside each unit cell [see Eqs. (6) and (8)] and by using the definition of the effective index, we get the following expressions for the conversion efficiencies:

$$\begin{aligned} \eta^+ &= \frac{2\omega^2 (d^{(2)}L)^2}{\varepsilon_0 c^3} G_A^+ I_\omega^{\text{input}} \\ &\quad \times \frac{\left(\exp \left[-N \frac{2\omega L}{c} \beta_{\text{eff}}^{2\omega} \right] - \exp \left[-N \frac{2\omega L}{c} \beta_{\text{eff}}^\omega \right] \right)^2 + 4 \exp \left[-N \frac{2\omega L}{c} (\beta_{\text{eff}}^\omega + \beta_{\text{eff}}^{2\omega}) \right] \sin^2 \left(N \frac{2\omega L}{c} (n_{\text{eff}}^{2\omega} - n_{\text{eff}}^\omega) \right)}{\left(\exp \left[-\frac{2\omega L}{c} \beta_{\text{eff}}^{2\omega} \right] - \exp \left[-\frac{2\omega L}{c} \beta_{\text{eff}}^\omega \right] \right)^2 + 4 \exp \left[-\frac{2\omega L}{c} (\beta_{\text{eff}}^\omega + \beta_{\text{eff}}^{2\omega}) \right] \sin^2 \left(\frac{2\omega L}{c} (n_{\text{eff}}^{2\omega} - n_{\text{eff}}^\omega) \right)}, \\ \eta^- &= \frac{2\omega^2 (d^{(2)}L)^2}{\varepsilon_0 c^3} G_A^- I_\omega^{\text{input}} \\ &\quad \times \frac{\left(1 - \exp \left[-N \frac{2\omega L}{c} (\beta_{\text{eff}}^\omega + \beta_{\text{eff}}^{2\omega}) \right] \right)^2 + 4 \exp \left[-N \frac{2\omega L}{c} (\beta_{\text{eff}}^\omega + \beta_{\text{eff}}^{2\omega}) \right] \sin^2 \left(N \frac{2\omega L}{c} (n_{\text{eff}}^\omega - n_{\text{eff}}^{2\omega}) \right)}{\left(1 - \exp \left[-\frac{2\omega L}{c} (\beta_{\text{eff}}^\omega + \beta_{\text{eff}}^{2\omega}) \right] \right)^2 + 4 \exp \left[-\frac{2\omega L}{c} (\beta_{\text{eff}}^\omega + \beta_{\text{eff}}^{2\omega}) \right] \sin^2 \left(\frac{2\omega L}{c} (n_{\text{eff}}^\omega - n_{\text{eff}}^{2\omega}) \right)}, \end{aligned} \quad (10)$$

where G_A^\pm are form or structure factors of the building block A : $G_A^\pm = (1/L) \int_0^L f(z) [\Phi_{\omega,A}^\pm(z)]^2 \Phi_{2\omega,A}^\mp(z) dz$, where $f(z)$ is the dimensionless profile of the nonlinear grating, i.e., $d^{(2)}(z) = d^{(2)} f(z)$, $\Phi_{\omega,A}^+(z)$ and $\Phi_{2\omega,A}^\mp(z)$ are the linear modes of the building block A at frequencies ω and 2ω , respectively, while the superscripts $+$ and $-$ refer, respectively,

to LTR and/or RTL modes. In Appendix A, we provide the mathematical details that bring about Eq. (10).

Before going any further, it is important to clarify a crucial point of our approach, and that is the issue of absorption. To arrive at Eq. (10), we have assumed that both the FF and the SH fields are tuned to spectral zones of the

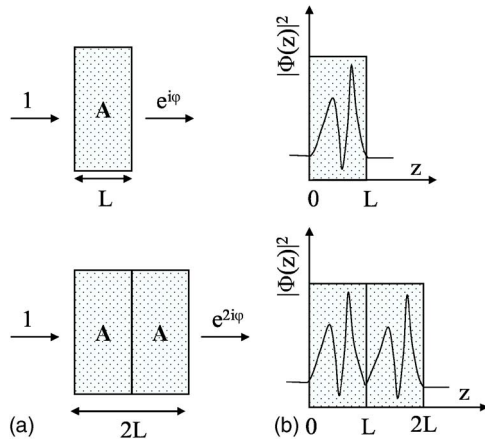


Fig. 1. Schematic of the behavior of the transmission and of the field localization on a transmission resonance when we double the original structure A. (a) transmission, (b) square modulus of the field $|\Phi(z)|^2$.

building block where the reflectivity is zero, i.e., $r=0$. This hypothesis is, of course, always satisfied at all transmission resonances of nonabsorbing structures, where $T=1$ and $R=0$. In the case of nonzero absorption, at resonance the condition $r=0$ is only *approximately* satisfied, depending on the amount of absorption considered. In that case, Eqs. (12) and (13) still describe the process well, provided the condition $|r/t| \ll 1$ is satisfied. Although at first sight the condition $|r/t| \ll 1$ might seem too restrictive, in reality it is not, because as we will see in the next section, it also holds for cases where absorption is small but significant. On the other hand, cases where absorption is high and the condition $|r/t| \ll 1$ ceases to be valid, are of little or no interest because the generation process is inefficient. Note that in any case one can resort to our Eq. (9), which, as we already stated, is valid in general.

Let us now emphasize the significance and the implications of Eq. (10), which represents the main result of this paper. First, the above formulas elucidate in an unambiguous way the two salient physical mechanisms that play key roles in the enhancement of the SH generation process in multilayered, finite structures, that is to say, mode and phase matching. The structure factors G_A^\pm are related to the mode matching, i.e., how well the FF and SH field overlap over the building block A, while the terms $\sin^2[N(2\omega L/c)[(n_{\text{eff}}^{2\omega} + n_{\text{eff}}^\omega)/2]]$ retain information on how well the SH process maintains itself after adding N building blocks. In other words, we gain intimate knowledge about the coherence length and its link to the real part of the effective index, n_{eff} .

Another important aspect worth noting is that the detrimental role played by the absorption is automatically encapsulated in the imaginary part of the effective index, β_{eff} . We also note that for $N=1$, the only quantity that matters for the SH conversion efficiency is mode matching over the building block A, i.e., the structure factors G_A^\pm .

To analyze in some detail the consequences of Eq. (10), let us discuss the case of no absorption. For any finite, nonabsorbing structure, it can be easily demonstrated using time reversal symmetry arguments (i.e., $t_\omega = t_\omega^*$, when $r=0$) that the phase of the transmission function t at the

transmission resonances takes on values that are integer multiples of π , i.e., $\varphi = m_\omega \pi$, where m_ω is an integer. m_ω is univocally determined by imposing the conditions that $\varphi(\omega)$ be a continuous function of ω , and that $\varphi \rightarrow 0$ when $\omega \rightarrow 0$. Now, in this case the effective index has no imaginary part and its expression is $n_{\text{eff}}^\omega = (c/\omega L)m_\omega \pi$. We have $(2\omega L/c)[(n_{\text{eff}}^{2\omega} + n_{\text{eff}}^\omega)/2] = (m_{2\omega} + 2m_\omega)(\pi/2)$. By substituting the previous expression into Eq. (10), and by taking into account that

$$\begin{aligned} \sin((2\omega L/c)(n_{\text{eff}}^{2\omega} + n_{\text{eff}}^\omega)) \\ &= \sin((m_{2\omega} + 2m_\omega)(\pi/2)) \\ &= \sin((m_{2\omega} - 2m_\omega)(\pi/2) + 2m_\omega \pi) \\ &= \sin((m_{2\omega} - 2m_\omega)(\pi/2)) \\ &= \sin((2\omega L/c)(n_{\text{eff}}^{2\omega} - n_{\text{eff}}^\omega)), \end{aligned}$$

we obtain

$$\eta^\pm = \frac{2(\omega d^{(2)}l)^2}{\varepsilon_0 c^3} G_A^\pm \frac{\sin^2(\Delta k_{\text{eff}} NL/2)}{N^2 \sin^2(\Delta k_{\text{eff}} L/2)} I_\omega^{\text{input}}, \quad (11)$$

where $\Delta k_{\text{eff}} = (2\omega/c)(n_{\text{eff}}^{2\omega} - n_{\text{eff}}^\omega)$. If we now write the conversion efficiency for a nonabsorbing bulk material of length $l=NL$ (Ref. 24):

$$\eta = \frac{2(\omega d^{(2)}l)^2}{n_\omega^2 n_{2\omega} \varepsilon_0 c^3} \sin^2(\Delta k l/2) I_\omega^{\text{input}}. \quad (12)$$

Comparing Eqs. (11) and (12), we immediately realize that the role played by the function $\sin^2(\Delta k l/2)$ in the case of bulk material is now played by the term $[\sin^2(\Delta k_{\text{eff}} NL/2)/N^2 \sin^2(\Delta k_{\text{eff}} L/2)]$. Equation (11) represents the general expression for SH conversion efficiency for *any kind* of nonabsorbing building block A repeated N times, assuming that both the FF and SH frequency are tuned at the transmission resonances of the building block. Equation (11) tells us that the SH generation process in the case of no absorption can be reduced to two sub cases: (1) $(m_{2\omega} - 2m_\omega) = 2p$ or $\Delta k_{\text{eff}} = 2p\pi/L$ for p any integer, including $p=0$ ($\Delta k_{\text{eff}}=0$).

In this case, from Eq. (11) we find that the conversion efficiency takes the following form:

$$\eta^\pm = \frac{2(\omega d^{(2)}NL)^2}{\varepsilon_0 c^3} G_A^\pm I_\omega^{\text{input}}. \quad (13)$$

This means that the conversion efficiency scales as the square of the total length of the structure $(NL)^2$, analogous to bulk material in perfect phase matching, and therefore the coherence length of the process is infinite, i.e., $l_c \rightarrow \infty$.

It is interesting and important to note that an infinite coherence length *does not* necessarily correspond to the case of perfect effective phase matching, as would be the case for SH generation in a bulk material. This means that every time the effective k -vector mismatch is $\Delta k_{\text{eff}} = 2p\pi/L$ with p an integer, the coherence length is infinite. The case $p=0$, i.e., $\Delta k_{\text{eff}}=0$, is just one of the cases in which the coherence length is infinite.

(2) $(m_{2\omega} - 2m_\omega) = 2p+1$ or $\Delta k_{\text{eff}} = (2p+1)\pi/L$ for p any integer, including $p=0$.

In the case at hand, we obtain from Eq. (17):

$$\eta^{\pm} = \frac{(1 - (-1)^N)(\omega d^{(2)}L)^2}{\varepsilon_0 c^3} G_{A\omega}^{\pm \text{input}}. \quad (14)$$

The SH conversion efficiency does not scale now as the square of the total length of the structure, but on the contrary it reaches the maximum of $\eta_{\text{MAX}}^{\pm} = [2(\omega d^{(2)}L)^2/\varepsilon_0 c^3] G_{A\omega}^{\pm \text{input}}$ for $N=1, 3, 5, \dots$; while it has a minimum $\eta_{\text{MIN}}^{\pm}=0$ for $N=2, 4, 6, \dots$. Therefore, the SH conversion efficiency as a function of the number of periods oscillates between a maximum value and 0. Now, the coherence length in a bulk material is the distance between two consecutive maxima of the conversion efficiency plotted as a function of the length of the material. Then, analogous to the coherence length of bulk materials, in the case analyzed the coherence length of the interaction is two times the length L of the building block A , i.e., $l_c=2L$.

This is an important result, which in short tells us that the coherence length for a structure made by the repetition of *any kind* of nonabsorbing building block of length L with *arbitrary* index profile can assume only two values, either $l_c \rightarrow \infty$ or $l_c=2L$, provided that both the FF and SH fields are tuned at the transmission resonances, i.e., where $T=1$, of the building block.

3. NUMERICAL EXAMPLES FOR 1D PHOTONIC CRYSTALS

The results obtained in the previous sections apply, regardless of the nature of the building block. However, here we numerically study the particular case in which building block A is itself made by repeating M times an elementary cell composed of two different materials, i.e., it is in the form of a 1D, finite, photonic crystal.

As a first example, let us consider a building block A composed of $M=20$ periods, nonabsorbing, alternating quarter-wave and half-wave layers of air ($\lambda/4$), and a generic dielectric material of refractive index $n(\lambda/2n)$, as in Refs. 5 and 6. The details of the structure are given in the caption of Fig. 2. The FF is tuned at the first transmission resonance near the first-order band edge of the structure, while the SH is tuned at the second transmission resonance near the second-order band edge. These tuning conditions correspond to perfect effective phase matching, i.e., $\Delta k_{\text{eff}}=0$, as expounded in Ref. 5. In Fig. 2, we plot the transmission spectrum of the building block, i.e., $N=1$, and of the structure made by repeating the building block $N=2$ and $N=3$ times.

For the $M=20$ -period structure (short-dashed curve), the pump frequency (ω_p) is tuned at the first transmission resonance to the left of the first bandgap, which corresponds to the 19th transmission resonance [Fig. 2(a)]. In turn, the SH ($2\omega_p$) is tuned to the second transmission resonance, also to the left of the second bandgap, so that the SH field coincides with the 38th transmission peak [Fig. 2(b)]. When we repeat the building block $N=2$ times, i.e., we pass from a $M=20$ -period to a $N^*M=40$ -period structure, the relative tuning of both the pump and the SH “move away” from their respective bandgaps, and as a result of geometrical dispersion the pump and SH fre-

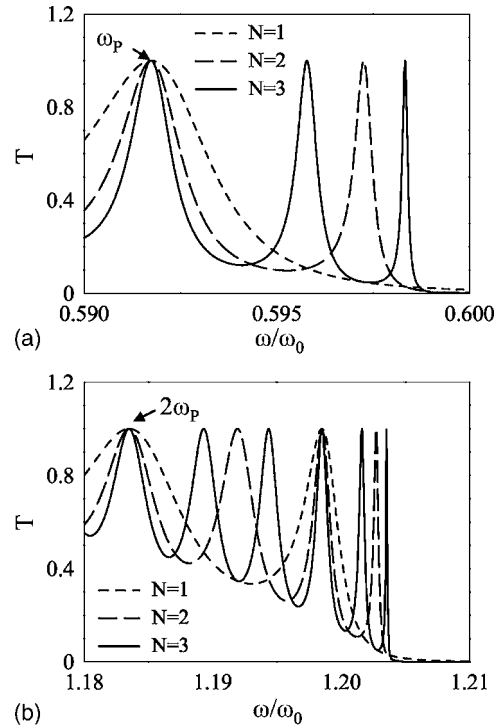


Fig. 2. Transmission (T) versus normalized frequency ω/ω_0 for a building block repeated N times, $\omega_0=2\pi c/\lambda_0$, and λ_0 is a reference wavelength. The building block is composed by $M=20$ -period alternating layers of air ($n_1=1$) and a generic dielectric material ($n_2=1.42857$ at pump frequency, ω_p) of thickness, respectively, $d_1=\lambda_0/4n_1$ and $d_2=\lambda_0/2n_2$. The dielectric material is assumed to have a linear dispersion between the pump and the SH frequency with the refractive index at the SH frequency $n_2(2\omega)=1.5178$. (a) Transmission near the low-frequency side of the first bandgap. (b) Transmission near the low-frequency side of the second bandgap. The arrows indicate the tuning of the FF and the SH frequency.

quencies are now found at the 38th and 76th transmission resonances, respectively (dashed curve). In a similar way, when the building block is repeated $N=3$ times, i.e., $N^*M=60$ -period structure, the pump frequency moves to the 57th transmission peak, while, the SH frequency shifts to the 114th transmission peak (solid curve). In Figs. 3 and 4, we show the real and the imaginary parts of the effective index, respectively, for the same structures considered in Fig. 2. The short-dashed curve refers to the $M=20$ -period structure, the dashed curve corresponds to the $N^*M=40$ -period structure, and the solid curve indicates the $N^*M=60$ -period structure. The figures confirm that the effective index has the same value for all these structures, both at the FF and at SH, as already demonstrated in the previous paragraph.

The structure just described belongs to the category analyzed in subcase (1), which predicts an infinite coherence length and a conversion efficiency that scales as the square of the total length of the structure. In fact, those predictions are confirmed in Fig. 5, where the conversion efficiency has been numerically calculated as a function of the number N of repetitions of the building block. The conversion efficiency scales as the square of the total length of the structure, i.e., as $(NL)^2$, exactly as predicted by Eq. (13). It is worth mentioning that, for 1D PCs N^6 and N^4 , scaling laws have been predicted in the past, see

Refs. 6 and 25, respectively. However, both cases refer to Bragg stacks made by N -time repetition of an elementary cell composed of two different layers. The N^6 and N^4 scaling laws are basically linked to the high field localization of the pump field available at the band-edge transmission resonances. Of course, a retuning of the FF at the band-edge transmission resonances is required in order to take advantage of the high field localization. This means, among other things, that the effective index of the structure at the FF and SH changes with N . Those aspects make the N^6 and N^4 scaling laws completely different from the N^2 scaling law that we find in this paper. First of all, our results have a more general validity because the only requirement is that the reflection function must be zero, no matter what the internal structure of the building block can be. In fact, in order to avoid confusion, we have used the terminology “building block” instead of “elementary cell,” because the latter is usually linked to Bragg stacks. Second, and more important, in our case there is no retuning of the FF, as we have already made clear at the beginning of the paper. In other words, the frequency of the pump field is kept constant while the number of building blocks is increasing, and moreover the dispersion properties of the building block are not changed.

So far we have numerically demonstrated that in the case of perfect phase matching $\Delta k_{eff}=0$, the conversion efficiency grows quadratically with the length of the structure. However, according to our theory, the perfect phase-

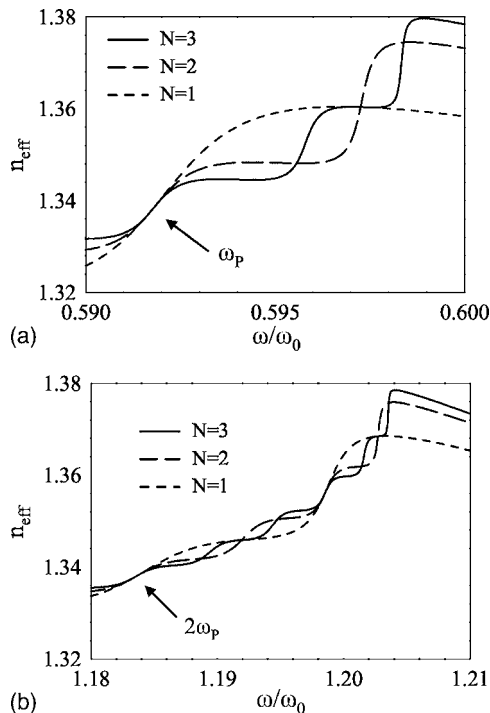


Fig. 3. Real part of the effective refractive index (n_{eff}) versus normalized frequency for N repetitions of the building block described in the caption of Fig. 2. (a) n_{eff} near the low-frequency side of the first bandgap. (b) n_{eff} transmission near the low-frequency side of the second bandgap. Note that at the transmission resonances the effective indexes of the structures are equal. The arrows indicate the tuning of the FF and the SH frequency. In this case, we have the perfect phase-matching condition, $\Delta k_{eff}=0$.

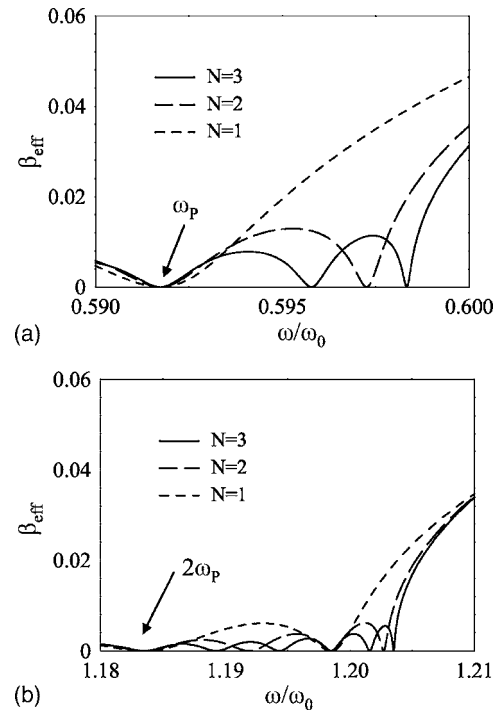


Fig. 4. Same as in Fig. 3 for the imaginary part of the effective index (β_{eff}).

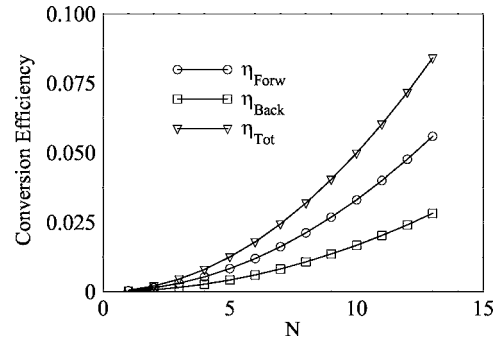


Fig. 5. Forward (circles), backward (squares), and total (triangles) conversion efficiency versus number of repetition (N) of the building block described in Fig. 2. The input intensity of the pump field is 100 MW/cm^2 and the quadratic coupling coefficient is $d^{(2)}=10 \text{ pm/V}$. The structure exists in perfect phase-matching conditions, $\Delta k_{eff}=0$. Note that the conversion efficiency grows as the square of the number of repetition, i.e., as the square of the total length and therefore the coherence length is infinite.

matching condition is only a special case for which this happens (in general, Δk_{eff} must be an even multiple of π/L .) In Fig. 6, we report the conversion efficiency as a function of the number of repetitions N in the case of a building block very similar to the one we have previously considered. Namely, we have adjusted the linear dispersion of the dielectric material in order to retune the SH to the fourth transmission resonance instead of the second (see inset of Fig. 6). In this case we have $\Delta k_{eff}=2\pi/L$, and once again the conversion efficiency scales as the square of the total length of the structure, as predicted.

In Fig. 7, we report the conversion efficiency as a function of the number of repetitions N in the case of a building block having $M=20$ periods, composed of alternating layers of air and a generic dielectric material having

thicknesses $\lambda/2(\text{air})-\lambda/4n$, respectively, similar to the structure studied in Ref. 16. In this case, the FF is tuned to the first transmission resonance near the first bandgap of the building block, while the SH is found at the first transmission resonance near the second bandgap, resulting in a effective phase mismatch of $\Delta k_{\text{eff}} = \pi/L$ (see inset of Fig. 7). Therefore the structure falls into the category analyzed in subcase (2). The numerical results shown in Fig. 7 confirm that in this case the coherence length of the structure is $l_c = 2L$, as predicted by Eq. (20). In Fig. 8, we compare the SH conversion efficiency of Fig. 7 with the SH conversion efficiency generated from a structure that has the same elementary cell of the structure described in Fig. 7. However, in this case the refractive index at the SH is slightly different, so that the SH is now tuned at the

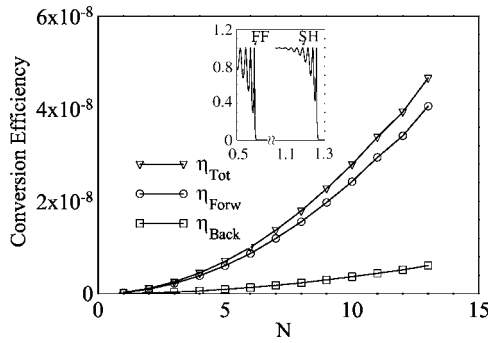


Fig. 6. Forward (circles), backward (squares), and total (triangles) conversion efficiency versus number of repetition (N) of the building block described in Fig. 2, with the difference that this time the dispersion of the dielectric material is adjusted in order to have the SH tuned at the fourth transmission resonance near the second band edge of the building block (see inset). The input intensity of the pump field is 100 MW/cm^2 and the quadratic coupling coefficient is $d^{(2)} = 10 \text{ pm/V}$. The mismatch term is an even multiple of π/L , $\Delta k_{\text{eff}} = 2\pi/L$. Note that again the conversion efficiency grows as the square of the number of repetition, and again the coherence length is infinite.

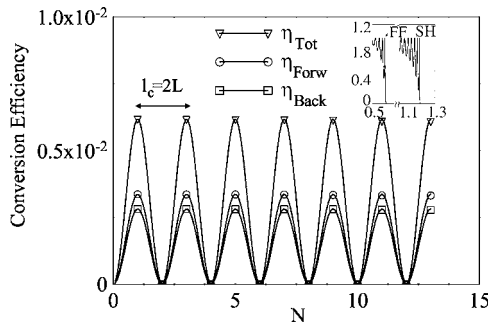


Fig. 7. Forward (circles), backward (squares), and total (triangles) conversion efficiency versus number of repetition (N) of a building block made by $M=20$ -period alternating layers of air ($n_1=1$) and a generic dielectric material ($n_2=1.42857$ at the pump frequency ω_p) of thickness, respectively, $d_1=\lambda_0/2n_1$ and $d_2=\lambda_0/4n_2$. The dispersion of the dielectric material is adjusted in order to have the SH tuned at the first transmission resonance near the second band edge of the building block (see inset). This tuning condition corresponds to an effective phase mismatch of $\Delta k_{\text{eff}} = \pi/L$, where L is the total length of the building block. In this case, the coherence length of the process is $l_c = 2L$. The input intensity of the pump field is 100 MW/cm^2 and the quadratic coupling coefficient is $d^{(2)} = 10 \text{ pm/V}$. Inset: Transmission versus ω/ω_0 for the building block. The arrows indicate the tuning of the FF and SH fields.

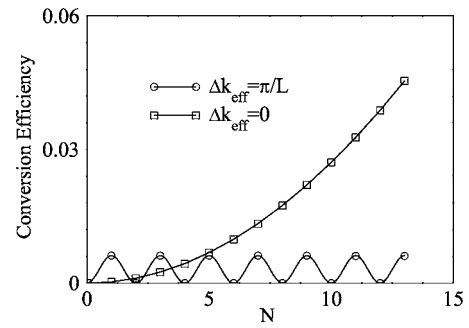


Fig. 8. Comparison between the total conversion efficiency of Fig. 7 when $\Delta k_{\text{eff}} = \pi/L$ (circles) and the total conversion efficiency generated from a structure identical to that described in Fig. 7, except that the dispersion is slightly different in order to tune the SH at the second transmission resonance near the second band edge so that $\Delta k_{\text{eff}} = 0$ (squares).

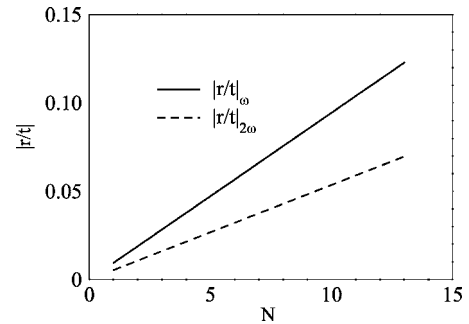


Fig. 9. Ratio of the reflection (r) over the transmission (t) versus the number of repetitions (N) of the building. The building block is the one described in the caption for Fig. 2, with the difference that this time the dielectric material is assumed to be absorbing, with an extinction coefficient $\beta = 5 \times 10^{-5}$.

second transmission resonance near the second band edge, i.e., in perfect phase matching.

As a fourth example, we will consider an absorbing case. Our building block is again based on the building block already considered in our first example, but with the addition of an extinction coefficient (β) of 5×10^{-5} . The effective index at the FF as well as the effective index at the SH is now a complex number: $n_{e,\omega} = 1.33803 + i2.20148 \times 10^{-4}$, and $n_{e,2\omega} = 1.33786 + i7.88932 \times 10^{-5}$. We expect our theory to be valid as long as the ratio $|r/t| \leq 10^{-2}$. In Fig. 9, we plot $|r/t|$ as a function of the number of repetitions of the building block. The value of the ratio increases with the number of repetitions, becoming significantly large above $N=5$. In Fig. 10, we plot the conversion efficiencies as a function of the number of repetitions. The dashed curves are the numerical results calculated according to Eq. (9), while the solid curves are the theoretical predictions according to Eq. (11). We can safely state that after five repetitions the theory and the numerical results begin to diverge, as expected.

4. CONCLUSIONS

In this paper, we have analytically discussed the role played by the effective index, the effective phase-matching conditions, and by the form factors, i.e., the overlap integrals, for SH generation in finite, multilayered structures. We have also clarified the meaning of co-

herence length of the process, and how it is related to the effective phase-matching condition. Our analytical results suggest that for nonabsorbing structures, the coherence length becomes infinite $l_c \rightarrow \infty$ when $\Delta k_{eff} = 2p\pi/L$, or it takes on the value of $l_c = 2L$ when $\Delta k_{eff} = (2p+1)\pi/L$ (L is the length of the building block, and p any integer including zero), provided that both FF and SH are tuned at the transmission resonances of the building block, as summarized by Eqs. (13) and (14). In the case of a building block made of an absorbing material, the real and imaginary parts of the effective index play an important role that determines the dynamics of the process. On the other hand, for structures composed of only one building block, the dynamics of SH generation is entirely governed by the form factors, i.e., by the overlap integrals over the structure, obviating the need for the evaluation of the effective index, as Eq. (10) suggests for the case where $N=1$.

APPENDIX A

In this appendix, we derive the analytical expression for SH conversion efficiency, i.e., Eq. (10) of the main text. The electric field at the FF (E_ω) and at the SH ($E_{2\omega}$) must satisfy the following system of nonlinear, coupled differential equations:

$$\begin{aligned} \frac{d^2 E_\omega}{dz^2} + \frac{\omega^2 \varepsilon_\omega(z) E_\omega}{c^2} &= -2 \frac{\omega^2}{c^2} d^{(2)}(z) E_\omega^* E_{2\omega}, \\ \frac{d^2 E_{2\omega}}{dz^2} + \frac{(2\omega)^2 \varepsilon_{2\omega}(z) E_{2\omega}}{c^2} &= -\frac{(2\omega)^2}{c^2} d^{(2)}(z) E_\omega^2. \end{aligned} \quad (A1)$$

In the undepleted pump approximation, Eq. (A1) can be written as

$$\begin{aligned} \frac{d^2 E_\omega}{dz^2} + \frac{\omega^2 \varepsilon_\omega(z) E_\omega}{c^2} &= 0, \\ \frac{d^2 E_{2\omega}}{dz^2} + \frac{(2\omega)^2 \varepsilon_{2\omega}(z) E_{2\omega}}{c^2} &= -\frac{(2\omega)^2}{c^2} d^{(2)}(z) E_\omega^2. \end{aligned} \quad (A2)$$

Equations (A2) admit the following solutions:

$$E_\omega(z) = A\Phi_\omega^+(z) + B\Phi_\omega^-(z),$$

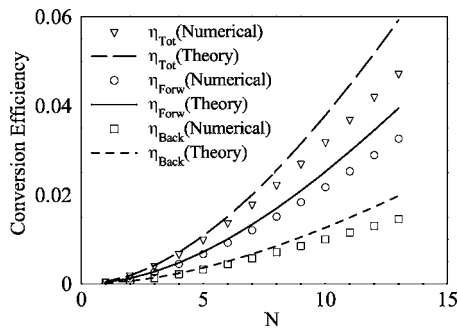


Fig. 10. Forward (circles), backward (squares), and total (triangles) conversion efficiency versus number of repetition (N) of the building block described in Fig. 9. The curves represent the prediction made with our theory. The input intensity of the pump field is 100 MW/cm^2 and the quadratic coupling coefficient is $d^{(2)} = 10 \text{ pm/V}$.

$$E_{2\omega}(z) = -\frac{(2\omega)^2}{c^2} \int_0^l G_{2\omega}(\xi, z) d^{(2)}(\xi) E_\omega^2(\xi) d\xi, \quad (A3)$$

where Φ_ω^+ and Φ_ω^- are the RTL and LTR propagating modes of the structure,²² respectively, at frequency ω . A and B are complex coefficients that have the physical dimensions of an electric field. These coefficients are uniquely determined by the boundary conditions. In the special case of LTR incidence, B is zero, while A is the magnitude of the electric field of the pump at the first interface. On the other hand, in the case of RTL incidence, A is zero, while B is the magnitude of the electric field at the last interface. We will study only the case of LTR incidence (i.e., $B=0$). In Eq. (A3), $l = NL$ is the length of the structure and $G_{2\omega}$ is the Green's function at frequency 2ω (Refs. 21–23):

$$G_{2\omega}(z, \xi) = \frac{1}{2ik_0^2 t_{2\omega}} \begin{cases} \Phi_{2\omega}^-(z) \Phi_{2\omega}^+(\xi), & z < \xi \\ \Phi_{2\omega}^+(z) \Phi_{2\omega}^-(\xi), & z > \xi \end{cases}, \quad (A4)$$

where $t_{2\omega}$ is the transmission of the whole structure at frequency 2ω and k_0^2 is the vacuum wave vector at frequency 2ω .

Taking into account Eqs. (A4) and Eqs. (A3), we find for a LTR incident pump the following expressions for the electric fields:

$$\begin{aligned} E_\omega(z) &= A\Phi_\omega^+(z), \\ E_{2\omega}(z) &= -\frac{(2\omega)^2}{c^2} \frac{A^2}{2ik_0^2 t_{2\omega}} \left[\Phi_{2\omega}^+(z) \int_0^z \Phi_{2\omega}^-(\xi) d^{(2)}(\xi) (\Phi_\omega^+(\xi))^2 d\xi \right. \\ &\quad \left. + \Phi_{2\omega}^-(z) \int_z^l \Phi_{2\omega}^+(\xi) d^{(2)}(\xi) (\Phi_\omega^+(\xi))^2 d\xi \right]. \end{aligned} \quad (A5)$$

In the plane-wave regime, the conversion efficiency η of a process is defined by the ratio of the intensity of the generated wave and the intensity of the pump. Moreover, a forward η^+ and backward η^- conversion efficiencies can be defined without ambiguity:

$$\eta = \eta^+ + \eta^- = \frac{I_{2\omega, \text{Forward}}^{\text{output}} + I_{2\omega, \text{Backward}}^{\text{output}}}{I_\omega^{\text{input}}}, \quad (A6)$$

where $I_{2\omega, \text{Backward}}^{\text{output}} = (\frac{1}{2})\varepsilon_0 c |E_{2\omega}(0)|^2$ is the intensity of the SH field generated in the backward (–) direction, $I_{2\omega, \text{Forward}}^{\text{output}} = (\frac{1}{2})\varepsilon_0 c |E_{2\omega}(L)|^2$ is the intensity of the SH field in the forward direction (+), and $I_\omega^{\text{input}} = (\frac{1}{2})\varepsilon_0 c |A|^2$ is the intensity of the pump beam incident from LTR.

From Eqs. (A5) and (A6), we find the following expression for the forward and the backward conversion efficiencies:

$$\eta^+ = \frac{2\omega^2 l^2}{\varepsilon_0 c^3} \left| \frac{1}{l} \int_0^l d^{(2)}(z) [\Phi_\omega^+(z)]^2 \Phi_{2\omega}^-(z) dz \right|^2 I_\omega^{\text{input}}, \quad (A7a)$$

$$\eta^- = \frac{2\omega^2 l^2}{\varepsilon_0 c^3} \left| \frac{1}{l} \int_0^l d^{(2)}(z) [\Phi_\omega^+(z)]^2 \Phi_{2\omega}^+(z) dz \right|^2 I_\omega^{\text{input}}. \quad (\text{A7b})$$

Now, because we are supposing that our structure is made by repeating the building block N times, we can separate the integral into a sum of N integrals, each carried out over a unit cell A :

$$\eta^+ = \frac{2\omega^2 (NL)^2}{\varepsilon_0 c^3} \left| \frac{1}{NL} \sum_{k=0}^{N-1} \int_{kL}^{(k+1)L} d^2(z) \times [\Phi_\omega^+(z)]^2 \Phi_{2\omega}^-(z) dz \right|^2 I_\omega^{\text{input}}, \quad (\text{A8a})$$

$$\eta^- = \frac{2\omega^2 (NL)^2}{\varepsilon_0 c^3} \left| \frac{1}{NL} \sum_{k=0}^{N-1} \int_{kL}^{(k+1)L} d^2(z) \times [\Phi_\omega^+(z)]^2 \Phi_{2\omega}^+(z) dz \right|^2 I_\omega^{\text{input}}. \quad (\text{A8b})$$

If we suppose that the FF and SH fields are both tuned at transmission resonances of the building block A , then the FF and SH modes satisfy the translation properties already derived in Eqs. (6) and (8) of the main text, i.e., $\Phi_\omega^+(z+jL) = (t_{\omega,A})^j \Phi_\omega^+(z)$ and $\Phi_\omega^-(z+jL) = (t_{\omega,A})^{-j} \Phi_\omega^-(z)$, where $t_{\omega,A}$ is the transmission of the building block A at frequency ω . As a result, Eq. (A8) may be recast into the following form:

$$\eta^+ = \frac{2\omega^2 (L)^2}{\varepsilon_0 c^3} \left| \frac{1}{L} \int_0^L d^{(2)}(z) \times [\Phi_\omega^+(z)]^2 \Phi_{2\omega}^-(z) dz \right|^2 \left| \sum_{k=0}^{N-1} (t_{\omega,A}^2 t_{2\omega,A}^{-1})^k \right|^2 I_\omega^{\text{input}}, \quad (\text{A9a})$$

$$\eta^- = \frac{2\omega^2 (L)^2}{\varepsilon_0 c^3} \left| \frac{1}{L} \int_0^L d^{(2)}(z) \times [\Phi_\omega^+(z)]^2 \Phi_{2\omega}^+(z) dz \right|^2 \left| \sum_{k=0}^{N-1} (t_{\omega,A}^2 t_{2\omega,A})^k \right|^2 I_\omega^{\text{input}}. \quad (\text{A9b})$$

Now, for $0 < z < L$, i.e., inside the first building block, we

have $\Phi_\omega^+(z) = \Phi_{\omega,A}^+(z)$ and $\Phi_{2\omega}^+(z) = \Phi_{2\omega,A}^+(z)$, while $\Phi_{2\omega}^-(z) = t_{2\omega,A}^{N-1} \Phi_{\omega,A}^-(z)$, where $\Phi_{\omega,A}^+$ and $\Phi_{\omega,A}^-$ are the LTR and RTL modes, respectively, at the FF and SH frequencies calculated over the building block A . So by introducing the form or structure factors G_A^\pm of the building block A : $G_A^\pm = |(1/L) \int_0^L f(z) [\Phi_\omega^\pm(z)]^2 \Phi_{2\omega}^\mp(z) dz|^2$, where $f(z)$ is the dimensionless profile of the nonlinear grating, so that $d^{(2)} \times (z) = d^{(2)} f(z)$, Eq. (A9) takes the following form:

$$\eta^+ = \frac{2\omega^2 (d^{(2)} L)^2}{\varepsilon_0 c^3} G_A^+ |t_{2\omega,A}^{N-1}|^2 \left| \sum_{k=0}^{N-1} (t_{\omega,A}^2 t_{2\omega,A}^{-1})^k \right|^2 I_\omega^{\text{input}}, \quad (\text{A10a})$$

$$\eta^- = \frac{2\omega^2 (d^{(2)} L)^2}{\varepsilon_0 c^3} G_A^- \left| \sum_{k=0}^{N-1} (t_{\omega,A}^2 t_{2\omega,A})^k \right|^2 I_\omega^{\text{input}}. \quad (\text{A10b})$$

The sum in Eq. (A10) can be performed in a closed form using the power sum rule: $\sum_{k=0}^{N-1} a^k = (1-a^N)/(1-a)$ and the result is

$$\eta^+ = \frac{2\omega^2 (d^{(2)} L)^2}{\varepsilon_0 c^3} G_A^+ \left| \frac{t_{2\omega,A}^N - (t_{\omega,A}^2)^N}{t_{2\omega,A} - t_{\omega,A}^2} \right|^2 I_\omega^{\text{input}}, \quad (\text{A11a})$$

$$\eta^- = \frac{2\omega^2 (d^{(2)} L)^2}{\varepsilon_0 c^3} G_A^- \left| \frac{1 - (t_{\omega,A}^2 t_{2\omega,A})^N}{1 - t_{\omega,A}^2 t_{2\omega,A}} \right|^2 I_\omega^{\text{input}}. \quad (\text{A11b})$$

The last step is to substitute in to Eq. (A11) the expression of the transmission as a function of the effective index:

$$t_{\omega,A}^2 = T_{\omega,A} \exp[2i\varphi_{\omega,A}] = \exp[-2(\omega L/c)\beta_{\text{eff}}^\omega] \exp[i(2\omega L/c)n_{\text{eff}}^\omega]$$

and

$$t_{2\omega,A} = \sqrt{T_{2\omega,A}} \exp[i\varphi_{\omega,A}] = \exp[-(\omega L/c)\beta_{\text{eff}}^{2\omega}] \exp[i(2\omega L/c)n_{\text{eff}}^{2\omega}].$$

After some algebra, we obtain Eq. (10) of the main text:

$$\eta^+ = \frac{2\omega^2 (d^{(2)} L)^2}{\varepsilon_0 c^3} G_A^+ I_\omega^{\text{input}} \frac{\left(\exp\left[-N\frac{2\omega L}{c}\beta_{\text{eff}}^{2\omega}\right] - \exp\left[-N\frac{2\omega L}{c}\beta_{\text{eff}}^\omega\right] \right)^2 + 4 \exp\left[-N\frac{2\omega L}{c}(\beta_{\text{eff}}^\omega + \beta_{\text{eff}}^{2\omega})\right] \sin^2\left(N\frac{2\omega L}{c}(n_{\text{eff}}^{2\omega} - n_{\text{eff}}^\omega)\right)}{\left(\exp\left[-\frac{2\omega L}{c}\beta_{\text{eff}}^\omega\right] - \exp\left[-\frac{2\omega L}{c}\beta_{\text{eff}}^{2\omega}\right] \right)^2 + 4 \exp\left[-\frac{2\omega L}{c}(\beta_{\text{eff}}^\omega + \beta_{\text{eff}}^{2\omega})\right] \sin^2\left(\frac{2\omega L}{c}(n_{\text{eff}}^{2\omega} - n_{\text{eff}}^\omega)\right)}, \quad (\text{A12a})$$

$$\eta^- = \frac{2\omega^2(d^{(2)}L)^2}{\varepsilon_0 c^3} G_A^- I_{\omega}^{\text{input}} \frac{\left(1 - \exp\left[-N \frac{2\omega L}{c}(\beta_{\text{eff}}^{\omega} + \beta_{\text{eff}}^{2\omega})\right]\right)^2 + 4 \exp\left[-N \frac{2\omega L}{c}(\beta_{\text{eff}}^{\omega} + \beta_{\text{eff}}^{2\omega})\right] \sin^2\left(N \frac{2\omega L}{c}(n_{\text{eff}}^{\omega} - n_{\text{eff}}^{2\omega})\right)}{\left(1 - \exp\left[-\frac{2\omega L}{c}(\beta_{\text{eff}}^{\omega} + \beta_{\text{eff}}^{2\omega})\right]\right)^2 + 4 \exp\left[-\frac{2\omega L}{c}(\beta_{\text{eff}}^{\omega} + \beta_{\text{eff}}^{2\omega})\right] \sin^2\left(\frac{2\omega L}{c}(n_{\text{eff}}^{\omega} + n_{\text{eff}}^{2\omega})\right)}.$$
(A12b)

ACKNOWLEDGMENTS

N. Marttiucci and G. D'Aguanno thank the National Research Council for financial support.

N. Mattiucci's e-mail address is nadia.mattiucci@us.army.mil. G. D'Aguanno's e-mail address is giuseppe.daguanno@us.army.mil.

REFERENCES AND NOTES

1. J. D. Joannopoulos, R. D. Meade, and J. N. Winn, *Photonic Crystals: Molding the Flow of Light* (Princeton U. Press, 1995).
2. E. Yablonovitch, "Inhibited spontaneous emission in solid-state physics and electronics," *Phys. Rev. Lett.* **58**, 2059–2062 (1987).
3. S. John, "Strong localization of photons in certain disordered dielectric superlattices," *Phys. Rev. Lett.* **58**, 2486–2489 (1987).
4. N. Bloembergen and A. J. Sievers, "Nonlinear optical properties of periodic laminar structures," *Appl. Phys. Lett.* **17**, 483–486 (1970).
5. M. Centini, C. Sibilila, M. Scalora, G. D'Aguanno, M. Bertolotti, M. J. Bloemer, C. M. Bowden, and I. Nefedov, "Dispersive properties of finite, one dimensional photonic band gap structures: applications to nonlinear quadratic interactions," *Phys. Rev. E* **60**, 4891–4898 (1999).
6. M. Scalora, M. J. Bloemer, A. S. Manka, J. P. Dowling, C. M. Bowden, R. Viswanathan, and J. W. Haus, "Pulsed second-harmonic generation in nonlinear, one-dimensional, periodic structures," *Phys. Rev. A* **56**, 3166–3175 (1997).
7. A. V. Tarasishin, A. M. Zheltikov, and S. A. Magnitskii, "Matched second-harmonic generation of ultrashort laser pulses in photonic crystals," *JETP Lett.* **70**, 819–825 (1999).
8. C. De Angelis, F. Gringoli, M. Midrio, D. Modotto, J. S. Aitchison, and G. F. Nalesso, "Conversion efficiency for second-harmonic generation in photonic crystals," *J. Opt. Soc. Am. B* **18**, 348–351 (2001).
9. M. Midrio, L. Socci, and M. Romagnoli, "Frequency conversion in one-dimensional stratified media with quadratic nonlinearity," *J. Opt. Soc. Am. B* **19**, 83–88 (2002).
10. Y. Dumeige, P. Vidakovic, S. Sauvage, I. Sagnes, J. A. Levenson, C. Sibilila, M. Centini, G. D'Aguanno, and M. Scalora, "Enhancement of second-harmonic generation in a one-dimensional semiconductor photonic band gap," *Appl. Phys. Lett.* **78**, 3021–3024 (2001).
11. Y. Dumeige, I. Sagnes, P. Monnier, P. Vidakovic, I. Abram, C. Mériade, and J. A. Levenson, "Phase-matched frequency doubling at photonic band edge: efficiency scaling as the fifth power of the length," *Phys. Rev. Lett.* **89**, 043901 (2002).
12. H. Yang, P. Xie, S. K. Chan, Z. Q. Zhang, I. K. Sou, G. K. L. Wong, and K. S. Wong, "Efficient second harmonic generation from large band gap II-VI semiconductor photonic crystal," *Appl. Phys. Lett.* **87**, 131106 (2005).
13. M. Centini, G. D'Aguanno, M. Scalora, C. Sibilila, M. Bertolotti, M. J. Bloemer, and C. M. Bowden, "Simultaneously phase-matched enhanced second and third harmonic generation," *Phys. Rev. E* **64**, 046606 (2001).
14. Y.-H. Ye, D.-Y. Jeong, T. S. Mayer, and Q. M. Zhang, "Finite-size effect on highly dispersive photonic-crystal optical components," *Appl. Phys. Lett.* **82**, 2380–2383 (2003).
15. A. N. Vamivakas, B. E. A. Saleh, A. V. Sergienko, and M. C. Teich, "Theory of spontaneous parametric down-conversion from photonic crystals," *Phys. Rev. A* **70**, 043810 (2004).
16. M. Centini, G. D'Aguanno, L. Sciscione, C. Sibilila, M. Bertolotti, M. Scalora, and M. J. Bloemer, "Non-phase-matched enhancement of second-harmonic generation in multilayer nonlinear structures with internal reflections," *Opt. Lett.* **29**, 1924–1927 (2004).
17. G. D'Aguanno, M. Centini, M. Scalora, C. Sibilila, M. Bertolotti, M. J. Bloemer, and C. M. Bowden, "Generalized coupled-mode theory for $\chi^{(2)}$ interactions in finite multilayered structures," *J. Opt. Soc. Am. B* **19**, 2111–2121 (2002).
18. G. D'Aguanno, M. Centini, M. Scalora, C. Sibilila, M. Bertolotti, C. M. Bowden, and M. J. Bloemer, "Energy exchange properties during second-harmonic generation in finite one-dimensional photonic band-gap structures with deep gratings," *Phys. Rev. E* **67**, 016606 (2003).
19. G. D'Aguanno, M. Centini, M. Scalora, C. Sibilila, M. Bertolotti, E. Fazio, C. M. Bowden, and M. J. Bloemer, "Slowing light in $\chi^{(2)}$ photonic crystals," *Phys. Rev. E* **68**, 046613 (2003).
20. P. Yeh, *Optical Waves in Layered Media* (Wiley, 1988).
21. G. D'Aguanno, N. Mattiucci, M. Scalora, M. J. Bloemer, and A. M. Zheltikov, "Density of modes and tunneling times in finite, one-dimensional, photonic crystals: a comprehensive analysis," *Phys. Rev. E* **70**, 016612 (2004).
22. O. Di Stefano, S. Savasta, and R. Girlanda, "Mode expansion and photon operators in dispersive and absorbing dielectrics," *J. Mod. Opt.* **48**, 67–84 (2001).
23. N. Mattiucci, G. D'Aguanno, M. J. Bloemer, and M. Scalora, "Second-harmonic generation from a positive-negative index material heterostructure," *Phys. Rev. E* **72**, 066612 (2005).
24. A. Yariv and P. Yeh, *Optical Waves in Crystals* (Wiley, 1984), Chap. 12.4.
25. T. Ochiai and K. Sakoda, "Scaling law of enhanced second-harmonic generation in finite Bragg stacks," *Opt. Express* **13**, 9095–9114 (2005).